Nucleic Acids Research, 2001, Vol. 29, No. 14 **2963–2972**

Involvement of *Schizosaccharomyces pombe* Srs2 in cellular responses to DNA damage

Shao-Win Wang, Adele Goodwin, Ian D. Hickson and Chris J. Norbury*

Imperial Cancer Research Fund Molecular Oncology Laboratory, University of Oxford Weatherall Institute of Molecular Medicine, John Radcliffe Hospital, Oxford OX3 9DS, UK

Received April 30, 2001; Revised and Accepted June 5, 2001

ABSTRACT

In the budding yeast *Saccharomyces cerevisiae* the Srs2/RadH DNA helicase promotes survival after ultraviolet (UV) irradiation, and has been implicated in DNA repair, recombination and checkpoint signalling following DNA damage. A second helicase, Sgs1, is the *S.cerevisiae* homologue of the human BLM and WRN proteins, which are defective in cancer predisposition and/or premature ageing syndromes. *Saccharomyces cerevisiae* cells lacking both Srs2 and Sgs1 exhibit a severe growth defect. We have identified an Srs2 orthologue in the fission yeast *Schizosaccharomyces pombe*, and have investigated its role in responses to UV irradiation and inhibition of DNA replication. Deletion of fission yeast *srs2* caused spontaneous hyper-recombination and UV sensitivity, and simultaneous deletion of the *SGS1* homologue *rqh1* caused a severe growth defect reminiscent of that seen in the equivalent *S.cerevisiae* mutant. However, unlike in budding yeast, inactivation of the homologous recombination pathway did not suppress this growth defect. Indeed, the homologous recombination pathway was required for maintenance of normal fission yeast viability in the absence of Srs2, and loss of homologous recombination and loss of Srs2 contributed additively to UV sensitivity. We conclude that Srs2 plays related, but not identical, roles in the two yeast species.

INTRODUCTION

Eukaryotic cells engage a variety of protective responses following DNA damage. These include the activation of DNA repair and intracellular checkpoint signalling pathways, which serve to delay cell cycle progression while DNA damage persists. Genetic strategies, principally using the budding yeast *Saccharomyces cerevisiae* and the distantly related fission yeast *Schizosaccharomyces pombe*, have identified a large number of radiation sensitive (*rad*) mutants that are defective in one or more of these protective pathways. Such studies have provided an increasingly detailed view of the roles of the corresponding Rad proteins in DNA damage responses. Many of the *rad* gene products are required for DNA repair processes, specifically nucleotide excision repair (NER), recombinational repair, non-homologous end joining (NHEJ) and post-replication gap-filling. Other Rad proteins have primary roles in checkpoint responses. The DNA damage checkpoint components partially overlap with those of the S-M checkpoint, which delays progression into or through mitosis when chromosomal DNA is not fully replicated. The extent of this overlap is clearest in *S.pombe* where, following either DNA damage or inhibition of replication, a common set of 'checkpoint Rad' proteins transduce checkpoint signals, which are presumed to be generated following the detection of abnormal DNA structures (1,2). Defects in the checkpoint Rad pathway allow progression into mitosis in the absence of complete DNA replication or in the presence of DNA strand breaks, giving rise to a characteristic 'cut' (cell untimely torn) phenotype.

For several gene products the distinction between functions in DNA repair, in checkpoint arrest or in recovery from such arrest is not straightforward. This is the case for the product of the *SGS1* gene in *S.cerevisiae*, and that of *rqh1* (also known as *hus2*/*rad12*), its homologue in *S.pombe*. These non-essential genes encode DNA helicases that are of particular interest because their human counterparts BLM and WRN are mutated in Bloom's and Werner's syndromes, disorders characterised in part by increased cancer incidence and premature ageing (3). Sgs1 and Rqh1 are required for maintenance of normal levels of resistance to the DNA replication inhibitor hydroxyurea (HU), to UV light and to ionizing radiation (4–7). The radiation sensitivity of *sgs1*/*rqh1* mutants can be interpreted in terms of a role for the corresponding proteins in DNA repair (5,7). In *S.pombe* this repair pathway appears also to involve the checkpoint Rad proteins, together with their effector, the protein kinase Cds1, and the homologous recombination machinery (5). Sgs1, Rqh1 and BLM are also required to prevent unscheduled mitotic recombination, either in the presence of DNA replication inhibitors or in the absence of any perturbation (4,8,9).

In *S.cerevisiae*, a second DNA helicase, Srs2, appears to be functionally related to Sgs1. Like *sgs1* mutants, cells lacking Srs2 are sensitive to DNA damaging agents and display elevated levels of mitotic recombination (10). Furthermore, simultaneous deletion of *SRS2* (also known as *RADH*) and *SGS1* results in a dramatic reduction in cell viability (7,11). This has been attributed to a role for these helicases in DNA replication, a function also recently ascribed to the *Xenopus* BLM protein (11,12). An alternative, but related, view is that

*To whom correspondence should be addressed. Tel: +44 1865 222415; Fax: +44 1865 222431; Email: norbury@icrf.icnet.uk

simultaneous loss of Sgs1 and Srs2 results in lethal levels of aberrant recombination. This view is supported by the observation that inactivation of the homologous recombination pathway by deletion of the *RAD51* gene substantially suppresses the growth defect seen in *sgs1 srs2* strains (7,13).

Although Srs2 is structurally related to bacterial DNA helicases (14), orthologues of *S.cerevisiae SRS2* have not so far been described in other eukaryotes. Here, we describe the identification and characterisation of the *S.pombe* gene most closely related to *SRS2*. Our data lead us to conclude that this fission yeast gene is required for maintenance of normal levels of resistance to DNA damaging agents, and that in some aspects its function resembles *S.cerevisiae SRS2*. Nonetheless, genetic interactions between *S.pombe srs2* and the recombination pathway differ from those of *SRS2* in *S.cerevisiae*, suggesting significant divergence of activity.

MATERIALS AND METHODS

Database searches

Searches to identify Srs2-related sequences in *S.pombe* were performed using the Sanger Centre BLAST server (http://www.sanger.ac.uk/Projects/S_pombe/blast_server.shtml). Ψ-BLAST (http://www.ncbi.nlm.nih.gov/cgi-bin/BLAST/nph-psi_blast) searches were used to identify similarities between Srs2 and proteins in the Swiss-Prot database. The protein sequence alignment in Figure 1A was created using the PILEUP program (University of Wisconsin Genetics Computer Group) and displayed using MacBoxshade (written by Michael Baron: michael.baron@bbsrc.ac.uk).

Fission yeast strains and methods

Conditions for growth, maintenance and genetic manipulation of fission yeast were as described previously (15). A complete list of the strains used in this study is given in Table 1. Except where otherwise stated, strains were grown at 30°C in YPD or EMM2 medium with appropriate supplements. Where necessary, gene expression from the *nmt1* promoter was repressed by the addition of 5 μM thiamine to the growth medium.

Construction of the *ade6-M26/ade6-L469* stable diploid strain and measurement of mitotic recombination rates were performed exactly as described elsewhere (4).

Gene disruption and related techniques

The one-step disruption method was used, following PCR-mediated generation of the entire *ura4*$^+$ gene or kanMX cassette flanked by 80 bp segments from the 5′ and 3′ regions of the gene to be disrupted (16). Oligonucleotides used to generate disruption cassettes for *srs2*, *rad22* and *rad51* (SRS2A and B, R22A and B and R51A and B, respectively) are listed in Table 2. Following transformation of a diploid strain 428/429, ura$^+$ progeny were screened for the desired integration pattern by diagnostic PCR using primer pairs spanning the presumptive recombination sites (details of the additional primers used for this purpose are available from the authors on request). Frequencies of homologous recombination (i.e. successful targeted gene disruption) ranged from 9 to 80%. Meiosis and sporulation were induced by plating onto malt extract agar, and tetrad dissection was performed with an MSM micromanipulator (Singer Instruments, UK) as described by Moreno *et al.* (15). Construction of the *nmt1* promoter replacement and chromosomally HA epitope-tagged *srs2* strains (*nmt1:HAsrs2* and *srs2:HA*) was accomplished by an analogous method using primers NMTA and B and TAGA and B, respectively (Table 2). Deletion of *rqh1* was described previously (17).

Table 1. *Schizosaccharomyces pombe* strains used in this study

Strain	Genotype	Source
HM123	*h⁻ leu1-32*	Laboratory stock
428h	*h⁻ ade6-M210 leu1-32 ura4-D18*	Laboratory stock
429h	*h⁺ ade6-M216 leu1-32 ura4-D18*	Laboratory stock
srs2Δ	*h⁻ srs2::ura4⁺ ade6-M216 leu1-32 ura4-D18*	This study
srs2Δ (LEU2)	*h⁻ srs2::LEU2 ade6-M210 leu1-32 ura4-D18*	This study
nmt1:HAsrs2	*h⁻ nmt1:HAsrs2 kanMX6 ade6-M216 leu1-32 ura4-D18*	This study
srs2:HA	*h⁻ srs2:HA kanMX6 ade6-M216 leu1-32 ura4-D18*	This study
L469	*h⁻ leu1-32 ade6-L649*	T. Enoch
M26	*mat2-102 his3-27 ade6-M26*	T. Enoch
srs2Δ (L469)	*h⁻ srs2::ura4⁺ ade6-L649 leu1-32 ura4-D18*	This study
srs2Δ (M26)	*mat2-102 srs2::ura4⁺ ade6-M26 his3-27 ura4-D18*	This study
rqh1Δ	*h⁻ rqh1::ura4⁺ leu1-32 ura4-D18*	A.M. Carr
rqh1Δ (kanMX6)	*h⁺ rqh1::kanMX6 ade6-M216 leu1-32 ura4-D18*	Laboratory stock
rhp51Δ	*h⁻ rhp51::ura4⁺ ade6-M216 leu1-32 ura4-D18*	This study
rhp54Δ	*h⁺ rhp54::ura4⁺ ade6-704 leu1-32 ura4-D18*	A. Pastink
rad13Δ	*h⁻ rad13::ura4⁺ ade6-704 leu1-32 ura4-D18*	A.M. Carr
rad22Δ	*h⁺ rad22::kanMX6 ade6-M210 leu1-32 ura4-D18*	This study
top3Δ (AG8Sp)	*h⁺/h⁻ top3::ura4⁺/top3⁺ ade6-M216/ade6-M210 leu1-32/leu1-32 ura4-D18/ura4-D18 his7/his7*	Laboratory stock

Table 2. Oligonucleotides used in this study

Name	Sequence (5′-3′)
SRS2A	TACTAAGAAATTGCAAGTGTTGTTTTCAACTAAATAAGGGTTGATCTTCTAAA TTATTTCACCTATGCTATGCTTTCGTTAAATCCCACTGGCTATATGT
SRS2B	TAATTTTGTTACTGACAATGACCATCTGCCTTCATCTACCGGTGTTTGCGAAT TTTGTGATAACGTATTATATCTTTCTAAATTCTAAATGCCTTCTGAC
R22A	GGTACCTGTCCATGTGCACACAGCTAATATACTGCTTCATATAAGCTAGAAGG GATGTCTCGGATCCCCGGGTTAATTAA
R22B	GGCGGAAAGAGGATCAAGGTGGCAGGCAGCCTTTTGCCGGATAGCAATTGAAT ATTCAGACAATTATTACATCGATGAATTCGAGCTCG
R51A	ACCTAATCTCTCTTTTCTTTAATAATATAAAAAACTTTTCAATTTCAGAATAG CGATAATTTCGTGCTTAACAAGTTATAAAATCCCACTGGCTATATGT
R51B	ATCACATACATATCTATCCTTACAAACTCATCCCATAGAATTTGCAAAATAAT AAATAAAAATGAAACGATACTAAAATAAATTCTAAATGCCTTCTGAC
NMTA	TACTAAGAAATTGCAAGTGTTGTTTTCAACTAAATAAGGGTTGATCTTCTAAA TTATTTCACCTATGCTATGCTTTCGTTGAATTCGAGCTCGTTTAAAC
NMTB	TGAGTATACTTATGAGGACTCTGAACACTAATCCTTTGTTCTTCATTCAGAAA CTTCAAGTATGATGATTTCGTTTCCATGCACTGAGCAGCGTAATCTG
TAGA	CAAATACTAAGGTCGCGAGTGCCCGTCCTGCTGGTTCGAGAAAACGATTGGGT GTAAGGCTACGAGTTTCACGAATGTTACGGATCCCCGGGTTAATTAA
TAGB	TAATTTTGTTACTGACAATGACCATCTGCCTTCATCTACCGGTGTTTGCGAAT TTTGTGATAACGTATTATATCTTTCTAGAATTCGAGCTCGTTTAAAC

Antibodies and immunoblotting

Immunoblotting was performed essentially as described elsewhere (18) using Mini-Protean electrophoresis equipment

(Bio-Rad, Hercules, CA) and a semi-dry transfer apparatus (Hoefer) in conjunction with Hybond ECL membranes (Amersham Pharmacia, UK). Proteins were detected using enhanced chemiluminescence (ECL, Amersham) following 1 h incubations at room temperature with the respective primary and horseradish peroxidase-conjugated anti-mouse antibodies (Sigma, Poole, UK). The mouse anti-influenza haemagglutinin (HA) monoclonal HA-11 (BAbCO, Berkeley, CA) was used at 1 µg/ml for detection of HA-tagged Srs2. Cdc2 was detected using the mouse monoclonal antibody Y100 (generated by Dr J. Gannon and kindly provided by Dr H. Yamano).

Microscopy and flow cytometry

Cells fixed in 70% ethanol were re-hydrated and stained with 4′,6-diamidino-2-phenylindole (DAPI) before examination by fluorescence microscopy. Images were acquired using a Zeiss Axioskop equipped with an Axiocam cooled CCD camera and Axiovision software (Carl Zeiss Ltd, Welwyn Garden City, UK) and were assembled using Adobe Photoshop. For flow cytometric analysis, cells were fixed at a density of 10^7/ml in 70% ethanol at 4°C overnight. Fixed cells were washed once with 50 mM sodium citrate buffer (pH 7), resuspended in the same buffer containing 100 µg/ml DNase-free RNase and incubated at 37°C overnight. After staining with propidium iodide (4 µg/ml final concentration), cells were analysed by flow cytometry (FACScan, Becton Dickinson, Oxford, UK) using a 488 nm laser. Red fluorescence (DNA) and forward light scatter (cell size) data were collected on linear scales for 10 000 cells for each strain and were analysed using CellQuest software.

RESULTS

Identification of the *S.pombe srs2* gene and protein

BLAST searches of the near-complete *S.pombe* genome database using the 1175 amino acid *S.cerevisiae* Srs2 protein sequence identified a single novel *S.pombe* gene (designated SPAC4H3.05) encoding a protein (Swiss-Prot accession number Q10213) significantly related to the query sequence throughout most of its length (27% amino acid identity, 40% similarity over a 698 amino acid region; Fig. 1A). Among all the putative ATP-dependent DNA helicases in the Swiss-Prot database, the hypothetical *S.pombe* protein sequence was most closely related to that of *S.cerevisiae* Srs2. We consequently refer to this *SRS2*-like *S.pombe* gene as *srs2*$^+$, in deference to the established *S.cerevisiae* nomenclature. The C-terminal regions of the two Srs2 sequences lacked significant similarity either to each other or to other known proteins.

The *srs2*$^+$ gene encodes a predicted protein of 887 amino acid residues, with a calculated molecular weight of 101 061. Homologous recombination with a PCR-generated fragment was used to place an HA epitope tag sequence in-frame with the 3′ end of the *srs2* open reading frame. Western blotting demonstrated the expression of the HA-tagged Srs2 protein, and indicated that there was no obvious change in the abundance or electrophoretic mobility of this protein after exposure of *S.pombe* cells to HU or the radiomimetic drug bleomycin (Fig. 1B). Consistent with the calculated molecular weight, HA-tagged Srs2 had a migration appropriate to a protein of just over 100 kDa.

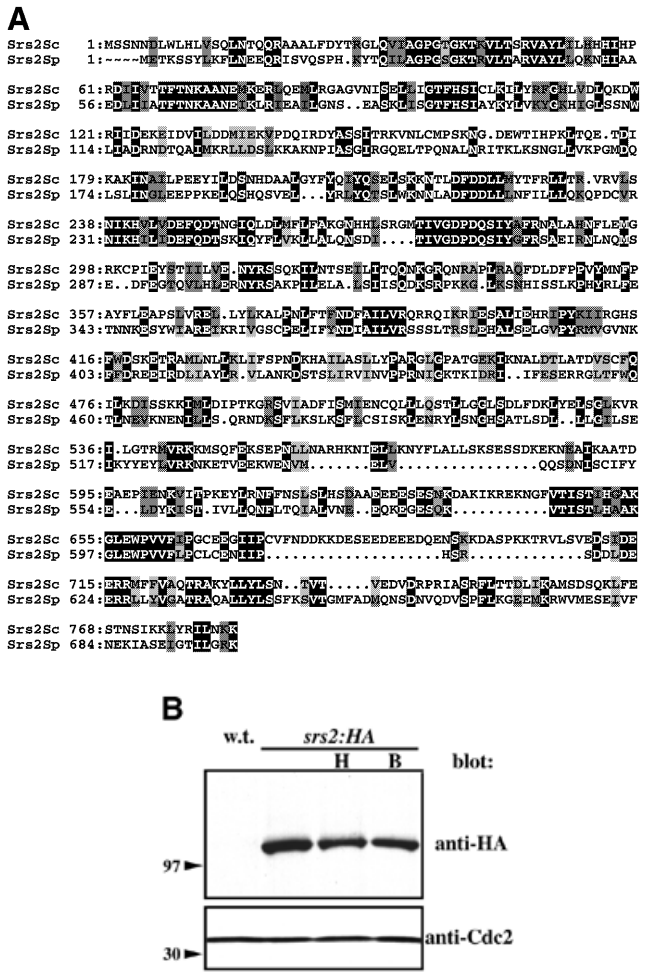

Figure 1. Srs2 is structurally conserved between *S.cerevisiae* and *S.pombe*. (**A**) An alignment of the amino acid sequences of budding yeast Srs2 (Srs2Sc; residues 1–782) and the fission yeast Srs2 protein described here (Srs2Sp; residues 1–698). White text on a black background indicates amino acid identity, black text on a shaded background indicates conservative amino acid substitutions. (**B**) Whole cell protein extracts were prepared from an untagged control (w.t.) strain or a genomic HA-tagged srs2 strain (*srs2:HA*; see Materials and Methods) grown to mid-exponential phase, and exposed to 10 mM hydroxyurea (H) for 4 h or 200 µg/ml bleomycin (B) for 2 h. The extracts were separated by SDS–PAGE and subjected to immunoblotting using anti-HA or anti-Cdc2 (loading control) antibodies, as indicated. The positions at which 97 and 30 kDa size markers migrated are also indicated.

Deletion of *srs2* causes hyper-recombination and sensitivity to DNA damage

As a first step towards determining the function of *srs2*$^+$ in *S.pombe*, one copy of the gene was replaced with the *ura4*$^+$ marker in a *ura4-D18* diploid strain and, after induction of meiosis, tetrads were dissected. Haploid ura$^+$ progeny segregated 2:2, indicating that the *srs2* gene is not essential for growth. The ura$^+$, *srs2*-deleted (*srs2*Δ) progeny had plating efficiencies and growth rates similar to those of their *srs2*$^+$ (ura$^-$) counterparts and to *rqh1*-deleted (*rqh1*Δ) cells (Fig. 2A and Table 3).

We next compared the sensitivites of *srs2*Δ and *rqh1*Δ cells to agents that inhibit DNA replication or induce DNA damage. *Schizosaccharomyces pombe srs2*Δ cells were mildly sensitive

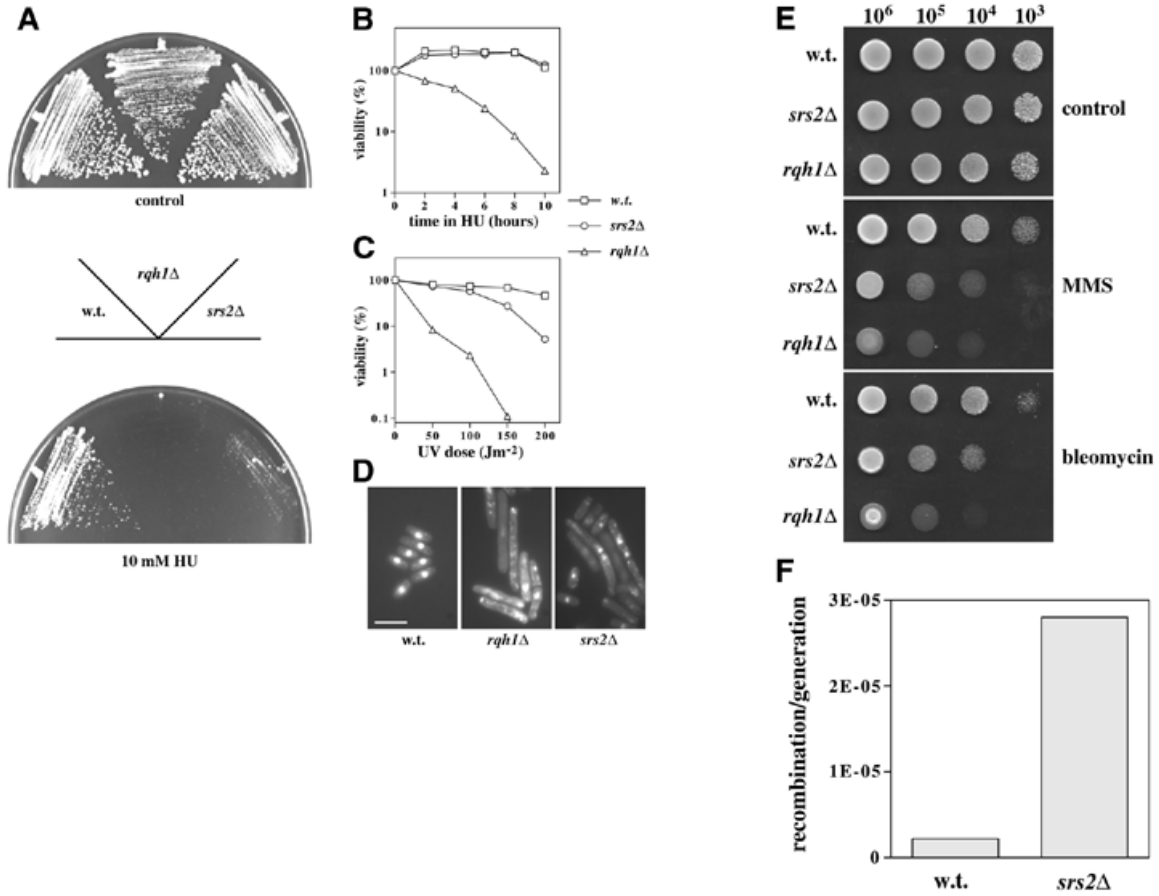

Figure 2. Characterisation of the *srs2*Δ phenotype; sensitivity to HU, UV, MMS or bleomycin, and elevated recombination rate. (**A**) A wild-type strain (HM123) and the single mutants *rqh1*Δ and *srs2*Δ were streaked in the positions shown onto YPD agar (control) or YPD agar containing 10 mM HU, as indicated. Plates were photographed after 4 days growth at 30°C. (**B**) The same strains were exposed to 10 mM HU in liquid culture for up to 10 h. Viability relative to that seen before addition of HU was measured by plating aliquots of each culture onto YPD agar plates and counting colony numbers after 4 days growth at 30°C. (**C**) Sensitivity of the same strains to UV was measured similarly by counting colony numbers after exposure to the indicated UV doses on YPD agar plates. (**D**) Cell and nuclear morphologies of *rqh1*$^+$ *srs2*$^+$ (HM123), *rqh1*Δ and *srs2*Δ strains were determined by fluorescence microscopy of DAPI-stained cells 14 h after exposure to 200 Jm^{-2} UV. Scale bar: 10 µm. (**E**) Ten-fold serial dilutions of these strains spanning the range from 10^6 to 10^3 cells, as indicated, were spotted onto YPD agar plates containing 0.005% MMS, 5 µg/ml bleomycin or neither drug (control). Plates were photographed after 3–5 days incubation at 30°C. (**F**) Recombination rates were measured in *srs2*$^+$ (HM123) and *srs2*Δ strains as described in Materials and Methods. Data are expressed as mean recombination frequency per generation.

to HU, although not as sensitive as *rqh1*Δ cells, as judged by continuous growth on agar containing HU (Fig. 2A). The *rqh1*Δ strain lost >90% cell viability by 8 h exposure to HU in liquid culture, as judged by colony formation (Fig. 2B). In contrast, there was no significant loss of viability in the *srs2*Δ strain after short-term HU treatment. The sensitivity of *srs2*Δ cells grown on agar containing HU therefore presumably reflects a requirement for Srs2 during continuous exposure to HU.

There was no significant loss of viability in the *srs2*Δ strain after exposure to 50 J/m^2 UV, a dose sufficient to cause a 90% loss of viability of *rqh1*Δ cells (Fig. 2C). At higher doses, *srs2*Δ cells were significantly UV sensitive (~90% loss of viability at 200 J/m^2) in comparison with a *srs2*$^+$ control, but were far less sensitive than *rqh1*Δ cells. Microscopic examination of cells 14 h after UV treatment (200 J/m^2) showed that wild-type controls had regained a normal morphology by this time (Fig. 2D). In comparison, UV-treated *srs2*Δ or *rqh1*Δ cells displayed a variety of defects, including cell elongation, aberrant nuclear morphology and unequal chromosome segregation. In some cases the highly elongated cells contained a single mass of chromatin bisected by a septum. In the case of *rqh1* mutants, this 'late cut' phenotype reflects failure to resume cell cycle progression faithfully after UV-induced cell cycle arrest, which explains the cell elongation (4). Both *rqh1*Δ and *srs2*Δ strains showed significant sensitivity to the alkylating agent methyl methanesulphonate (MMS) and to the radiomimetic drug bleomycin (Fig. 2E). In each case the *srs2*Δ strain displayed a sensitivity intermediate to those of the wild-type and *rqh1*Δ strains.

Sensitivity to DNA damage in *rqh1* and *sgs1* mutants is associated with elevated levels of mitotic recombination. In order to address whether or not the same is true for *srs2*Δ cells, *srs2*$^+$ and *srs2*Δ stable diploid strains were constructed containing the *ade6-M26* and *ade6-L469* heteroalleles. Reciprocal recombination or gene conversion between these alleles can lead to the generation of ade$^+$ progeny, and the frequency with which these arise therefore provides a convenient index of mitotic recombination rate (4). Using this approach, we found that the spontaneous recombination rate in the *srs2*Δ

Table 3. Growth characteristics of *srs2*Δ, *rqh1*Δ, *rhp51*Δ, *rad22*Δ and *rhp54*Δ strains

Strain	Doubling time (h)	Plating efficiency (%)
HM123 (wild-type)	2.3	98
*srs2*Δ	2.6	85
*rqh1*Δ	2.7	87
*srs2*Δ *rqh1*Δ	6.3	36
*rhp51*Δ	3.5	73
*rhp51*Δ *rqh1*Δ	3.8	58
*rhp51*Δ *srs2*Δ	4.8	43
*rhp51*Δ *srs2*Δ *rqh1*Δ	7.2	21
*rad22*Δ	4.0	48
*rad22*Δ *rqh1*Δ	7.5	10
*rhp54*Δ	3.8	64
*rhp54*Δ *rqh1*Δ	4.0	31

diploid strain was elevated ~12-fold with respect to the wild-type control (Fig. 2F).

Simultaneous deletion of *srs2* and *rqh1* causes a dramatic growth defect

As simultaneous mutation of budding yeast *SGS1* and *SRS2* results in lethality, we were interested to see whether there might be an analogous interaction between the corresponding genes in *S.pombe*. A diploid strain was constructed in which one allele of *srs2* was disrupted by the *ura4*$^+$ marker and one allele of *rqh1* was disrupted by the *kanMX6* cassette, conferring resistance to the neomycin analogue G418. Dissection of ascospores from this strain following induction of meiosis showed that, as expected, haploid segregants bearing either the *srs2::ura4*$^+$ or the *rqh1::kanMX6* allele were able to grow and form colonies normally. From 90 tetrads dissected, the numbers of *srs2*$^+$ *rqh1*$^+$, *srs2*Δ *rqh1*$^+$ and *srs2*$^+$ *rqh1*Δ segregant colonies visible after 3 days growth at 30°C were 78, 76 and 80, respectively. These numbers are close to the 90 that would be expected for independently segregating markers, and indicate that there was only a slight overall loss of spore viability attributable to heterozygosity at the *srs2* and *rqh1* loci in the diploid. In contrast, only 14 *srs2*Δ *rqh1*Δ segregant colonies were visible after 7 days growth, and these formed only extremely slowly growing microcolonies. Microscopic examination showed that many of the cells in these slowly growing colonies were highly elongated, suggesting that one or more aspects of cell cycle progression are defective when both Rqh1 and Srs2 are absent (Fig. 3A). DAPI staining of these cells showed that cell and nuclear morphologies were relatively normal in the *srs2*Δ and *rqh1*Δ single mutants, although some of the cells in each of these strains were somewhat elongated (Fig. 3B). In line with their poor overall viability, the *srs2*Δ *rqh1*Δ double mutants exhibited a variety of aberrant morphologies, including highly elongated cells, 'cut' cells and others with apparently much reduced nuclear DNA content. The overall appearance of these cells was broadly similar to that of UV-treated *srs2*Δ or *rqh1*Δ single mutants (Fig. 2D). Flow

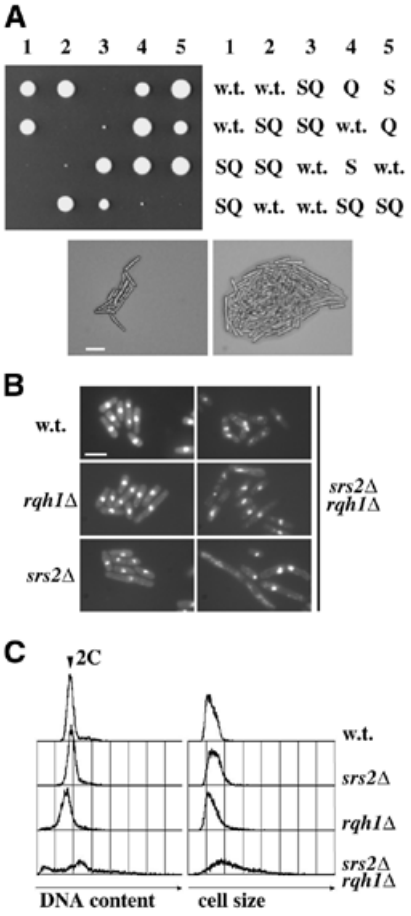

Figure 3. Genetic interaction between *srs2* and *rqh1*. (**A**) An h^+/h^- *srs2::ura4*$^+$/*srs2*$^+$ *rqh1::kanMX6*/*rqh1*$^+$ diploid [*srs2*Δ × *rqh1*Δ(kanMX6)] was induced to undergo meiosis and sporulation, and tetrads were microdissected onto YPD agar. Colonies resulting from five such tetrads were photographed after 7 days growth at 30°C (upper left). The genotypes of these segregants were determined by replica plating and are indicated schematically (upper right: w.t., *srs2*$^+$ *rqh1*$^+$; S, *srs2*Δ *rqh1*$^+$; Q, *srs2*$^+$ *rqh1*Δ; SQ, *srs2*Δ *rqh1*Δ). Micrographs of two representative *srs2*Δ *rqh1*Δ colonies, taken after 7 days growth at 30°C, are shown below (scale bar: 20 μm). (**B**) Fluorescence micrographs of DAPI-stained *srs2*$^+$ *rqh1*$^+$ (w.t.), *rqh1*Δ, *srs2*Δ and *srs2*Δ *rqh1*Δ cells (scale bar: 10 μm). (**C**) Flow cytometric analyses of propidium iodide-stained cells of the strains indicated. Histograms of DNA content (red fluorescence, left) and cell size (forward light scatter, right) derived from 10 000 cells are shown. The position corresponding to a 2C (G_2/M) DNA content is indicated (arrow). Note that the brevity of G_1 and the coincidence of S phase with cytokinesis result in the absence of a detectable 1C population in exponentially growing *S.pombe* cultures.

cytometric analysis confirmed that the DNA content and overall size of *srs2*Δ *rqh1*Δ cells were very variable in comparison with those of the corresponding single mutants (Fig. 3C). Some 17% of the *srs2*Δ *rqh1*Δ cells had little or no nuclear DNA as judged by this assay, compared with 0.17, 0.63 and 6.5% for wild-type, *srs2*Δ and *rqh1*Δ cells, respectively.

Deletion of *rhp51* does not suppress the growth defect of *srs2 rqh1* double mutants

A recent study showed that the loss of viability in *S.cerevisiae sgs1 srs2* strains can be partially suppressed by simultaneous loss of the homologous recombination function encoded by

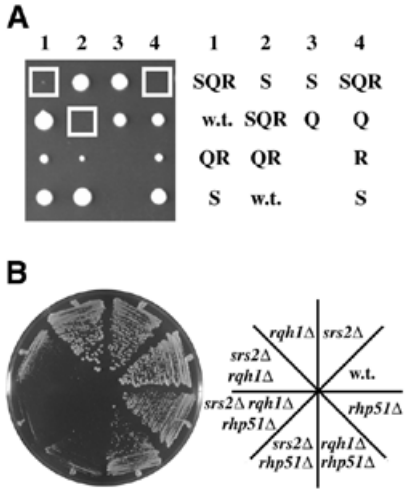

Figure 4. Deletion of *rhp51* fails to suppress the *srs2*Δ *rqh1*Δ growth defect. (**A**) An h^+/h^- *srs2::LEU2*/*srs2*$^+$ *rqh1::kanMX6*/*rqh1*$^+$ *rhp51*::*ura4*$^+$/*rhp51*$^+$ diploid was induced to undergo meiosis and sporulation, and tetrads were microdissected onto YPD agar. Colonies resulting from four such tetrads were photographed after 7 days growth at 30°C (left). The genotypes of these segregants were determined by replica plating and are indicated schematically (right: w.t., *srs2*$^+$ *rqh1*$^+$ *rhp51*$^+$; S, *srs2*Δ *rqh1*$^+$; Q, *srs2*$^+$ *rqh1*Δ; R, *rhp51*Δ; QR, *rqh1*Δ *rhp51*Δ; SQR, *srs2*Δ *rqh1*Δ *rhp51*Δ). The positions occupied by *srs2*Δ *rqh1*Δ *rhp51*Δ mutants are boxed (left). (**B**) The strains indicated (right) were streaked onto YPD agar and photographed (left) after 4 days growth at 30°C.

RAD51 (7). With this in mind, we investigated the effect of deletion of *rhp51*, the *S.pombe* orthologue of *RAD51* (19), on the viability of *srs2*Δ *rqh1*Δ cells. A diploid strain was constructed that was heterozygous for deletions of *srs2* (replaced in this case with the *LEU2* marker) *rqh1* (*kanMX6*) and *rhp51* (*ura4*$^+$). Following sporulation and dissection of tetrads, identification of the genotypes of the progeny showed that deletion of *rhp51* did not suppress the growth defect characteristic of *srs2*Δ *rqh1*Δ cells (Fig. 4A). On the contrary, *srs2*Δ *rqh1*Δ *rhp51*Δ cells were barely viable at all, with a longer doubling time and lower plating efficiency than those of an otherwise isogenic *srs2*Δ *rqh1*Δ mutant (Fig. 4B and Table 3). From 116 tetrads dissected, only five slowly growing *srs2*Δ *rqh1*Δ *rhp51*Δ microcolonies (and nine *srs2*Δ *rhp51*Δ colonies) were visible after 7 days growth at 30°C. In contrast, the numbers of *srs2*$^+$ *rqh1*$^+$ *rhp51*$^+$ and *srs2*Δ segregants (50 and 63, respectively) were close to the 58 expected in the case of three independently segregating markers ($116 \times 4/2^3$). The additional growth defect conferred by *rhp51* deletion was ascribed largely to a genetic interaction between *rhp51* and *srs2*. Deletion of *rqh1* in a *rhp51*Δ background resulted in a slightly increased doubling time and decreased plating efficiency in comparison with the *rhp51*Δ single mutant, but the effect of *srs2* deletion in this background was much more severe (Fig. 4B and Table 3). *srs2*Δ *rhp51*Δ double mutants grew at a similarly slow rate to that seen in *srs2*Δ *rqh1*Δ double mutants.

Homologous recombination is required for maintenance of viability in *srs2* and *rqh1* mutants

The genetic interaction between *srs2* and *rhp51* described above was investigated in further detail by examining the

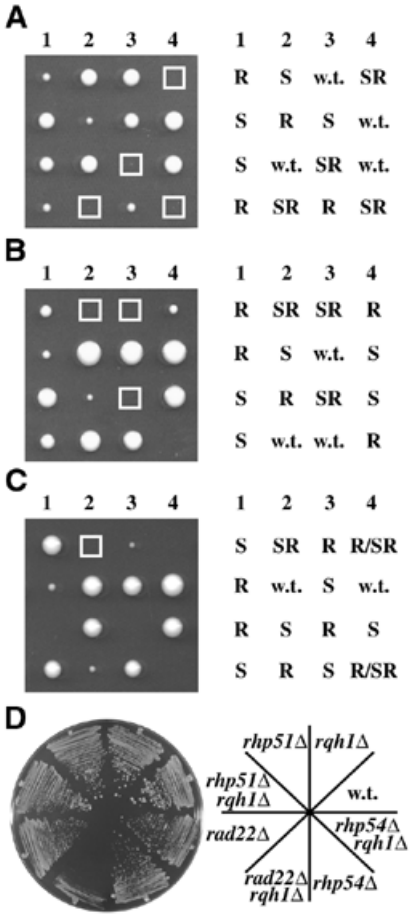

Figure 5. Genetic interactions between *srs2* and homologous recombination genes. (**A**–**C**) Tetrads derived from diploid strains of the following genotypes were microdissected onto YPD agar: h^+/h^- *srs2::LEU2*/*srs2*$^+$ *rhp51*::*ura4*$^+$/*rhp51* (A), h^+/h^- *srs2::ura4*$^+$/*srs2*$^+$ *rad22::kanMX6*/*rad22*$^+$ (B) and h^+/h^- *srs2::LEU2*/*srs2*$^+$ *rhp54::ura4*$^+$/*rhp54*$^+$ (C). Colonies resulting from four tetrads in each case were photographed after 7 days growth at 30°C. The genotypes of the segregants were determined by replica plating and are indicated schematically [right: w.t., *srs2*$^+$ *rqh1*$^+$ *rhp51*$^+$ *rad22*$^+$ *rhp54*$^+$; S, *srs2*Δ; R, *rhp51*Δ (A), *rad22*Δ (B) or *rhp54*Δ (C); SR, *srs2*Δ *rhp51*Δ (A), *srs2*Δ *rad22*Δ (B) or *srs2*Δ *rhp54*Δ (C)]. Boxes (left) indicate the positions of *srs2* double mutants with *rhp51*, *rad22* and *rhp54*, respectively. (**D**) The strains indicated (right) were streaked onto YPD agar and photographed (left) after 4 days growth at 30°C.

effect of combining *srs2*Δ with deletions of *rad22* or *rhp54* (*S.pombe* homologues of *S.cerevisiae RAD52* and *RAD54*, respectively), which like *rhp51* encode components of the homologous recombination pathway (19–22). Moreover, it was of interest to determine whether or not the lethality previously observed to result from combining *srs2* and *rad54* mutations in *S.cerevisiae* (23) would also be seen in *S.pombe*. Diploid strains heterozygous for deletion of *srs2* and for deletion of *rhp51*, *rad22* or *rhp54* were constructed (see Materials and Methods). Dissection of ascospores following induction of meiosis provided independent confirmation that there is a synthetic interaction between *srs2* and *rhp51* (Fig. 5A). Of 108 tetrads dissected from the *srs2*Δ *rhp51*Δ heterozygous diploid, only 13 spores gave rise to viable haploid *srs2*Δ *rhp51*Δ colonies (in contrast to the 108 that would be expected for a cross involving two unlinked

markers), and all of these grew very slowly. The severity of this synthetic effect with *srs2* was if anything even more extreme in the cases of *rad22* and *rhp54* (Fig. 5B and C), although spore viability was only 64% even in *rhp54*Δ single mutants. Of 108 tetrads dissected from the *srs2*Δ *rad22*Δ heterozygous diploid, and 126 dissected from the *srs2*Δ *rhp54*Δ heterozygous diploid, one and zero spores, respectively, gave rise to doubly mutant haploid microcolonies. Thus, *S.pombe* cells lacking Srs2 are dependent on the homologous recombination pathway for maintenance of viability.

Genetic interactions between *rqh1* and homologous recombination genes were also examined in further detail. An earlier study demonstrated that the UV sensitivities of *rqh1* and *rhp51* or *rhp54* mutants were not additive (5). Similarly, we found that *rqh1*Δ *rhp51*Δ and *rqh1*Δ *rhp54*Δ mutants grew only slightly more slowly than the single *rhp51*Δ mutant (Fig. 5D and Table 3), although their plating efficiencies were somewhat reduced. A much more pronounced synthetic interaction was seen on combining *rqh1*Δ with *rad22*Δ, however. Thus, the doubling time of a *rqh1*Δ *rad22*Δ strain was almost twice that of a *rad22*Δ single mutant, and the plating efficiency was decreased almost 5-fold (Fig. 5D and Table 3).

The epistatic relationship between *rqh1* and *rhp51*/*rhp54* with respect to UV sensitivity (5) has been interpreted in terms of an involvement of the products of these genes in a common pathway of DNA damage tolerance. The modest UV sensitivity of *srs2*Δ cells (Fig. 2C) and the synthetic interactions between *srs2* and homologous recombination genes in the absence of exogenous DNA damage (Fig. 5A–C) suggested that *srs2* is unlikely to participate in such a pathway, at least not to the same extent as *rqh1*. In line with this interpretation, the UV sensitivity conferred by *srs2* deletion was additive with that resulting from deletion of *rhp51*, required for recombinational repair, or *rad13*, which is essential for the NER pathway (Fig. 6). By these criteria it would appear that *srs2* is required for a pathway of UV damage repair that is neither the recombination pathway nor NER.

Overexpression of *srs2* cannot compensate for deletion of *rqh1*

If the predicted DNA helicase activity of Srs2 were functionally related to that of Rqh1, overexpression of Srs2 might be sufficient to suppress defects seen in the absence of Rqh1. To address this point, PCR-mediated gene disruption was used to replace the promoter of the *srs2* gene in its normal chromosomal context with the thiamine-repressible *nmt1* promoter, at the same time introducing an HA epitope tag sequence fused in-frame to the 5′ end of the *srs2* open reading frame (see Materials and Methods). Removal of thiamine from the medium led to readily detectable levels of HA-Srs2 after 16 h growth at 30°C (Fig. 7A). In addition to the full-length, HA-tagged protein, a number of smaller species were detected, the most prominent of which migrated at ~35 kDa. Since the epitope tag is at the N-terminus, these shorter species most likely represent degradation products. Comparison with levels of Srs2-HA expressed from the *srs2* promoter in its normal chromosomal context indicated that the *nmt1* promoter-driven gene was overexpressed ~15-fold in comparison with endogenous *srs2*, but haploid HA-Srs2-expressing cells were not UV sensitive, suggesting that the overproduced protein is functional (S.W.Wang and C.Norbury, unpublished results). This level of srs2 overexpression had no effect on the UV (Fig. 7B) or HU (Fig. 7C) sensitivity of a *rqh1*Δ strain, however, indicating that Srs2 is incapable of performing the function of Rqh1 in response to these agents.

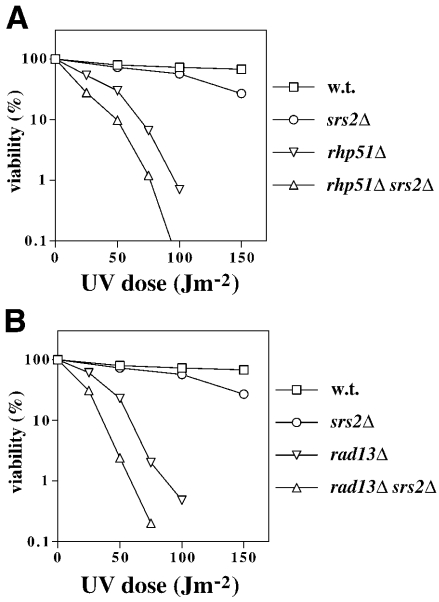

Figure 6. UV sensitivity resulting from *srs2* deletion is additive with that resulting from loss of homologous recombination or NER. (**A** and **B**) Sensitivity of the indicated strains to UV, relative to that seen without irradiation, was measured by counting colony numbers after 4 days growth at 30°C after exposure to the indicated UV doses on YPD agar plates.

Deletion of *srs2* fails to suppress the lethality of *top3* deletion

We showed previously that the lethality resulting from deletion of the *top3* gene encoding *S.pombe* topoisomerase III can be suppressed by deletion of *rqh1* (17,24). Similarly, in *S.cerevisiae*, deletion of *SGS1* suppresses the slow growth phenotype associated with *TOP3* deletion (25). If *srs2* were functionally related to *rqh1*, it might be expected that there would be an analogous genetic interaction between *srs2* and *top3*. On dissection of meiotic progeny from a diploid strain heterozygous for both *srs2* and *top3* deletions, none of the *top3::ura4*$^+$ spores was able to form colonies, regardless of the *srs2* genotype (data not shown). This lack of suppression of the *top3* phenotype by *srs2* deletion provides further evidence that the functions of *srs2* and *rqh1* are quite distinct.

DISCUSSION

Budding yeast *SRS2*/*RADH* acts with *SGS1* to suppress unscheduled recombination, and this function may be particularly important during DNA replication. Although structural and functional homologues of *SGS1* have been identified in eukaryotic species as diverse as yeasts and mammals, this report is the first to describe an *SRS2*-like gene function in any eukaryote other than *S.cerevisiae*. The completion of genome sequencing projects will make it possible to establish whether or not Srs2-like proteins exist in non-fungal eukaryotic species, but at this stage it has not been possible to identify clear

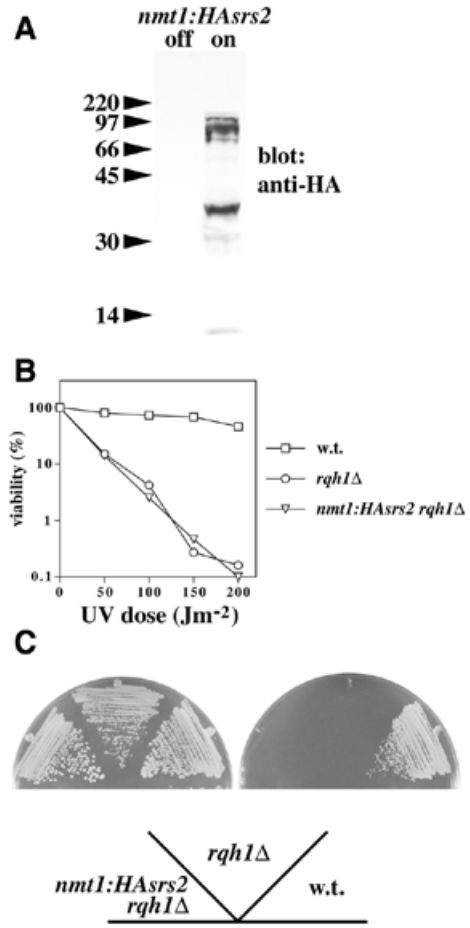

Figure 7. Overexpression of *srs2* fails to suppress the UV or HU sensitivity of a *rqh1*Δ mutant. (**A**) A strain (*nmt1:HAsrs2*) was constructed in which the endogenous *srs2* promoter is replaced by that of the thiamine-repressible *nmt1* gene, while incorporating an HA epitope tag sequence at the 5′ end of the *srs2* open reading frame (see Materials and Methods). Whole cell protein extracts were prepared from this strain grown to mid-exponential phase at 30°C in the presence of thiamine (off) or 16 h after the removal of thiamine (on), and were subjected to immunoblotting with an anti-HA antibody. (**B**) The UV sensitivities of the strains indicated were determined (as described in the legend to Fig. 6) 16 h after the removal of thiamine. (**C**) The same strains were streaked onto EMM2 agar (which lacks thiamine; plate on left) or EMM2 agar containing 10 mM HU (plate on right) and were photographed after 3–5 days growth at 30°C.

candidates among the available *Drosophila*, *Caenorhabditis* or human sequences (S.-W.Wang and C.Norbury, unpublished observations). The bacterial helicases most closely related to Srs2 (those of the PcrA family) are essential for DNA replication and repair (26). In *S.cerevisiae* an essential role for Srs2 and Sgs1 in chromosomal replication has also been proposed (11), but such a role is difficult to reconcile with the observation that the *srs2 sgs1* double mutant phenotype can be suppressed by simultaneous inactivation of the homologous recombination machinery (7). BLAST searches show that the *S.pombe* Srs2 amino acid sequence is significantly more similar to the bacterial members of this family than is *S.cerevisiae* Srs2. This could indicate that the common ancestral yeast contained two diverging Srs2 isoforms, only one of which is retained in each of the modern species. Other explanations, such as horizontal gene transfer from bacteria to an *S.pombe* ancestor, or more rapid sequence divergence in *S.cerevisiae*, cannot be ruled out however.

We have shown that Srs2 in *S.pombe* is required to maintain the normal level of resistance to UV irradiation, as is its counterpart in *S.cerevisiae*. The precise nature of this protective function is not yet clear. A cell cycle checkpoint role was proposed recently for *S.cerevisiae* Srs2 (27), but we currently have no indication that Srs2 has an analogous checkpoint function in *S.pombe*. Unlike the *S.cerevisiae* protein, *S.pombe* Srs2 was not phosphorylated in a checkpoint-dependent manner, as far as it was possible to judge by SDS–PAGE (Fig. 1B). In addition, *srs2*Δ cells, like *rqh1*Δ cells, became substantially elongated after UV irradiation (Fig. 2D), suggesting that establishment of the *S.pombe* DNA damage checkpoint is not Srs2 dependent. Instead, like Rqh1, Srs2 may be involved in a damage tolerance pathway that involves bypass of DNA damage by replication forks, reversal of cell cycle arrest and/or suppression of recombination (4,5). The substantially elevated level of spontaneous recombination seen in *srs2*Δ cells (Fig. 2F) would be compatible with such a role. Although elevated recombination was also seen on deletion of *rqh1*, this was not intrinsic, but dependent on inhibition of replication (4).

An alternative interpretation of the data would be that Srs2, like Rad6 and Rad18 in *S.cerevisiae*, functions in a post-replication gap-filling repair pathway. Indeed, the *SRS2* locus was first identified through dominant mutations capable of suppressing the UV sensitivities of *rad6* and *rad18* mutants (28). In this case, the hyper-recombination phenotype seen on *srs2* deletion could be attributable to an increased reliance on a recombinational pathway of post-replication repair, while simultaneous inactivation of this alternative pathway would give rise to the observed lethality or slow growth phenotype. A very recent study concluded that the synthetic lethality observed in *S.cerevisiae srs2 rad54* strains was attributable to activation of the DNA damage checkpoint (29). It will be interesting to determine whether or not inactivation of this checkpoint pathway can suppress the lethality seen in the equivalent double mutant in *S.pombe*.

Deletion of *rhp51* was reported previously to confer no additional sensitivity to UV on an *rqh1* deletion strain, suggesting that the two genes might act in a common pathway of DNA damage tolerance (5). In contrast, we showed that the UV sensitivities seen on deletion of *srs2* and *rhp51* are additive (Fig. 6A), suggesting that the UV-protective role of *srs2* does not operate through the recombinational repair pathway. Similarly, epistasis suggests that *srs2* acts independently of the NER pathway (Fig. 6B). It is possible that Srs2 acts in the NHEJ pathway of DNA repair in *S.pombe*, as has been reported recently for *S.cerevisiae* Srs2 (30), but at this stage it seems at least equally likely that its principal role is in a non-recombinational gap-filling pathway, as discussed above. Examination of the relationship between Rqh1, Srs2 and the homologous recombination machinery also revealed a specific requirement for *rad22*, but not other homologous recombination genes, in cells lacking *rqh1* (Fig. 5D and Table 3). Rad22/Rad52 homologues bind DNA ends and appear to act at an early stage in the homologous recombination pathway, interacting with Rad51 to promote homologous pairing (31–33). It is conceivable that Rqh1 and its homologues might act in

concert with Rad22/Rad52 at this early stage in recombination, potentially explaining the specific genetic interaction observed here between *rqh1* and *rad22*. The precise nature of any such interaction awaits further investigation.

While deletion of *srs2* on its own resulted in a comparatively minor growth defect, simultaneous deletion of *srs2* and *rqh1* was barely compatible with cell survival (Fig. 3 and Table 3). Thus, the function of Srs2 is conserved between *S.cerevisiae* and *S.pombe* at the level of genetic interaction with the sole RecQ family helicase in each yeast (Sgs1 and Rqh1, respectively). The analogous growth defect seen in *S.cerevisiae srs2 sgs1* mutants has been attributed to unrestrained recombination, as the phenotype can be suppressed by inactivation of the homologous recombination pathway (7). We have been unable to establish the underlying cause of the growth defect in *srs2*Δ *rqh1*Δ cells, partly because the strain itself grew so poorly, and partly because the growth defect is not suppressed by deletion of the homologous recombination gene *rhp51* (Fig. 4). Thus, despite our observation that spontaneous recombination is elevated in *srs2*Δ cells (Fig. 2F), we cannot implicate unscheduled spontaneous hyper-recombination in the *srs2*Δ *rqh1*Δ growth defect. Interpretation of the failure of *rhp51* deletion to suppress this growth defect is complicated by the fact that the *rhp51*Δ single mutant displays a growth defect, whereas no such defect has been described for the corresponding *S.cerevisiae* mutant. However, we observed a specific genetic interaction between *rhp51* and *srs2*, and a comparative lack of any such interaction between *rhp51* and *rqh1* (Figs 4B and 5A, and Table 3). These observations support the notion that the relationship between *srs2*/*SRS2* and the recombination pathway differs between *S.cerevisiae* and *S.pombe*.

In summary, we have identified the *S.pombe* orthologue of the *S.cerevisiae SRS2* gene. Several aspects of this gene function have been conserved during the interval of ~400 million years since the ancestors of these two yeasts diverged. In particular, *srs2* mutations in each yeast confer elevated levels of mitotic recombination and sensitivity to DNA damage, and are synthetically lethal with mutations in *rgh1*/*SGS1* and *rhp54*/*RAD54*. These functional similarities, along with the extensive sequence similarity (Fig. 1A), justify our conclusion that *srs2*$^+$ is the closest fission yeast counterpart of *SRS2*. In other respects, the *srs2*/*SRS2* function appears to have diverged. Thus, inactivation of the homologous recombination machinery, which is sufficient to suppress the lethality of *S.cerevisiae srs2 sgs1* mutants, was not capable of similarly suppressing the *srs2 rqh1* phenotype in *S.pombe*.

ACKNOWLEDGEMENTS

We are grateful to Tamar Enoch for providing the strains and methodology for measurement of recombination rates, to Albert Pastink and Tony Carr for providing *S.pombe* strains, and to Takashi Toda and members of the Molecular Oncology Laboratory for their helpful advice. This work was supported by the Imperial Cancer Research Fund.

REFERENCES

1. Carr,A.M. (1997) Control of cell cycle arrest by the Mec1sc/Rad3sp DNA structure checkpoint pathway. *Curr. Opin. Genet. Dev.*, **7**, 93–98.
2. O'Connell,M.J., Walworth,N.C. and Carr,A.M. (2000) The G2-phase DNA-damage checkpoint. *Trends Cell Biol.*, **10**, 296–303.
3. Chakraverty,R.K. and Hickson,I.D. (1999) Defending genome integrity during DNA replication: a proposed role for RecQ family helicases. *BioEssays*, **21**, 286–294.
4. Stewart,E., Chapman,C.R., Al-Khodairy,F., Carr,A.M. and Enoch,T. (1997) *rqh1*$^+$, a fission yeast gene related to the Bloom's and Werner's syndrome genes, is required for reversible S phase arrest. *EMBO J.*, **16**, 2682–2692.
5. Murray,J.M., Lindsay,H.D., Munday,C.A. and Carr,A.M. (1997) Role of *Schizosaccharomyces pombe* RecQ homolog, recombination and checkpoint genes in UV damage tolerance. *Mol. Cell. Biol.*, **17**, 6868–6875.
6. Frei,C. and Gasser,S.M. (2000) The yeast Sgs1p helicase acts upstream of Rad53p in the DNA replication checkpoint and colocalizes with Rad53p in S-phase-specific foci. *Genes Dev.*, **14**, 81–96.
7. Gangloff,S., Soustelle,C. and Fabre,F. (2000) Homologous recombination is responsible for cell death in the absence of the Sgs1 and Srs2 helicases. *Nature Genet.*, **25**, 192–194.
8. Heartlein,M.W., Tsuji,H. and Latt,S.A. (1987) 5-Bromodeoxyuridine-dependent increase in sister chromatid exchange formation in Bloom's syndrome is associated with reduction in topoisomerase II activity. *Exp. Cell Res.*, **169**, 245–254.
9. Watt,P.M., Hickson,I.D., Borts,R.H. and Louis,E.J. (1996) *SGS1*, a homologue of the Bloom's and Werner's syndrome genes, is required for maintenance of genome stability in *Saccharomyces cerevisiae*. *Genetics*, **144**, 935–945.
10. Aboussekhra,A., Chanet,R., Adjiri,A. and Fabre,F. (1992) Semidominant suppressors of Srs2 helicase mutations of *Saccharomyces cerevisiae* map in the *RAD51* gene, whose sequence predicts a protein with similarities to procaryotic RecA proteins. *Mol. Cell. Biol.*, **12**, 3224–3234.
11. Lee,S.K., Johnson,R.E., Yu,S.L., Prakash,L. and Prakash,S. (1999) Requirement of yeast *SGS1* and *SRS2* genes for replication and transcription. *Science*, **286**, 2339–2342.
12. Liao,S., Graham,J. and Yan,H. (2000) The function of *Xenopus* Bloom's syndrome protein homolog (xBLM) in DNA replication. *Genes Dev.*, **14**, 2570–2575.
13. Klein,H.L. (2000) A radical solution to death. *Nature Genet.*, **25**, 132–134.
14. Aboussekhra,A., Chanet,R., Zgaga,Z., Cassier-Chauvat,C., Heude,M. and Fabre,F. (1989) *RADH*, a gene of *Saccharomyces cerevisiae* encoding a putative DNA helicase involved in DNA repair. Characteristics of *radH* mutants and sequence of the gene. *Nucleic Acids Res.*, **17**, 7211–7219.
15. Moreno,S., Klar,A. and Nurse,P. (1991) Molecular genetic analysis of fission yeast *Schizosaccharomyces pombe*. *Methods Enzymol.*, **194**, 795–823.
16. Bähler,J., Wu,J.Q., Longtine,M.S., Shah,N.G., McKenzie,A.,III, Steever,A.B., Wach,A., Philippsen,P. and Pringle,J.R. (1998) Heterologous modules for efficient and versatile PCR-based gene targeting in *Schizosaccharomyces pombe*. *Yeast*, **14**, 943–951.
17. Goodwin,A., Wang,S.W., Toda,T., Norbury,C. and Hickson,I.D. (1999) Topoisomerase III is essential for accurate nuclear division in *Schizosaccharomyces pombe*. *Nucleic Acids Res.*, **27**, 4050–4058.
18. Ausubel,F.M., Brent,R., Kingston,R.E., Moore,D.D., Seidman,J.G., Smith,J.A. and Struhl,K. (1995) *Current Protocols in Molecular Biology*. John Wiley & Sons, Inc., New York, NY.
19. Muris,D.F.R., Vreeken,K., Schmidt,H., Ostermann,K., Clever,B., Lohman,P.H.M. and Pastink,A. (1997) Homologous recombination in the fission yeast *Schizosaccharomyces pombe*: different requirements for the *rhp51*$^+$, *rhp54*$^+$ and *rad22*$^+$ genes. *Curr. Genet.*, **31**, 248–254.
20. Schlake,C., Ostermann,K., Schmidt,H. and Gutz,H. (1993) Analysis of DNA repair pathways of *Schizosaccharomyces pombe* by means of swi-rad double mutants. *Mutat. Res.*, **294**, 59–67.
21. Ostermann,K., Lorentz,A. and Schmidt,H. (1993) The fission yeast *rad22* gene, having a function in mating-type switching and repair of DNA damages, encodes a protein homolog to Rad52 of *Saccharomyces cerevisiae*. *Nucleic Acids Res.*, **21**, 5940–5944.
22. Muris,D.F., Vreeken,K., Carr,A.M., Murray,J.M., Smit,C., Lohman,P.H. and Pastink,A. (1996) Isolation of the *Schizosaccharomyces pombe RAD54* homologue, *rhp54*$^+$, a gene involved in the repair of radiation damage and replication fidelity. *J. Cell Sci.*, **109**, 73–81.
23. Palladino,F. and Klein,H.L. (1992) Analysis of mitotic and meiotic defects in *Saccharomyces cerevisiae SRS2* DNA helicase mutants. *Genetics*, **132**, 23–37.

24. Maftahi,M., Han,C.S., Langston,L.D., Hope,J.C., Zigouras,N. and Freyer,G.A. (1999) The *top3*$^{+}$ gene is essential in *Schizosaccharomyces pombe* and the lethality associated with its loss is caused by Rad12 helicase activity. *Nucleic Acids Res.*, **27**, 4715–4724.
25. Gangloff,S., McDonald,J.P., Bendixen,C., Arthur,L. and Rothstein,R. (1994) The yeast type I topoisomerase Top3 interacts with Sgs1, a DNA helicase homolog: a potential eukaryotic reverse gyrase. *Mol. Cell. Biol.*, **14**, 8391–8398.
26. Petit,M.A., Dervyn,E., Rose,M., Entian,K.D., McGovern,S., Ehrlich,S.D. and Bruand,C. (1998) PcrA is an essential DNA helicase of *Bacillus subtilis* fulfilling functions both in repair and rolling-circle replication. *Mol. Microbiol.*, **29**, 261–273.
27. Liberi,G., Chiolo,I., Pellicioli,A., Lopes,M., Plevani,P., Muzi-Falconi,M. and Foiani,M. (2000) Srs2 DNA helicase is involved in checkpoint response and its regulation requires a functional Mec1-dependent pathway and Cdk1 activity. *EMBO J.*, **19**, 5027–5038.
28. Lawrence,C.W. and Christensen,R.B. (1979) Metabolic suppressors of trimethoprim and ultraviolet light sensitivities of *Saccharomyces cerevisiae* rad6 mutants. *J. Bacteriol.*, **139**, 866–887.
29. Klein,H.L. (2001) Mutations in recombinational repair and in checkpoint control genes suppress the lethal combination of *srs2*Δ with other DNA repair genes in *Saccharomyces cerevisiae*. *Genetics*, **157**, 557–565.
30. Hegde,V. and Klein,H. (2000) Requirement for the *SRS2* DNA helicase gene in non-homologous end joining in yeast. *Nucleic Acids Res.*, **28**, 2779–2783.
31. Parsons,C.A., Baumann,P., Van Dyck,E. and West,S.C. (2000) Precise binding of single-stranded DNA termini by human RAD52 protein. *EMBO J.*, **19**, 4175–4181.
32. Van Dyck,E., Stasiak,A.Z., Stasiak,A. and West,S.C. (1999) Binding of double-strand breaks in DNA by human Rad52 protein. *Nature*, **398**, 728–731.
33. Benson,F.E., Baumann,P. and West,S.C. (1998) Synergistic actions of Rad51 and Rad52 in recombination and DNA repair. *Nature*, **391**, 401–404.